Geochemistry Geophysics Geosystems G3

Article
Volume 12, Number 12
22 December 2011
Q12T11, doi:10.1029/2011GC003778
ISSN: 1525-2027

Published by AGU and the Geochemical Society

Origin of minor and trace element compositional diversity in anorthitic feldspar phenocrysts and melt inclusions from the Juan de Fuca Ridge

David T. Adams
U.S. Geological Survey, Denver Federal Center, MS 973, Denver, Colorado 80225, USA (dadams@usgs.gov)

Roger L. Nielsen and Adam J. R. Kent
Department of Geosciences, Oregon State University, 104 Wilkinson Hall, Corvallis, Oregon 97330-5506, USA (nielsenr@geo.oregonstate.edu; kentad@geo.oregonstate.edu)

Frank J. Tepley III
College of Oceanic and Atmospheric Sciences, Oregon State University, 104 COAS Admin Bldg., Corvallis, Oregon 97333-5503, USA (ftepley@coas.oregonstate.edu)

[1] Melt inclusions trapped in phenocryst phases are important primarily due to their potential of preserving a significant proportion of the diversity of magma composition prior to modification of the parent magma array during transport through the crust. The goal of this investigation was to evaluate the impact of formational and post-entrapment processes on the composition of melt inclusions hosted in high anorthite plagioclase in MORB. Our observations from three plagioclase ultra-phyric lavas from the Endeavor Segment of the Juan de Fuca Ridge document a narrow range of major elements and a dramatically greater range of minor and trace elements within most host plagioclase crystals. Observed host/inclusion partition coefficients for Ti are consistent with experimental determinations. In addition, observed values of D_{Ti} are independent of inclusion size and inclusion TiO_2 content of the melt inclusion. These observations preclude significant effects from the re-homogenization process, entrapment of incompatible element boundary layers or dissolution/precipitation. The observed wide range of TiO_2 contents in the host feldspar, and between bands of melt inclusions within individual crystals rule out modification of TiO_2 contents by diffusion, either pre-eruption or due to re-homogenization. However, we do observe comparatively small ranges for values of K_2O and Sr compared to P_2O_5 and TiO_2 in both inclusions and crystals that can be attributed to diffusive processes that occurred prior to eruption.

Components: 13,500 words, 7 figures, 1 table.

Keywords: crustal processes; magma transport; plagioclase.

Index Terms: 1021 Geochemistry: Composition of the oceanic crust; 1032 Geochemistry: Mid-oceanic ridge processes (3614, 8416).

Received 8 July 2011; **Revised** 31 October 2011; **Accepted** 6 November 2011; **Published** 22 December 2011.

This paper is not subject to U.S. copyright.
Published in 2011 by the American Geophysical Union.

Adams, D. T., R. L. Nielsen, A. J. R. Kent, and F. J. Tepley III (2011), Origin of minor and trace element compositional diversity in anorthitic feldspar phenocrysts and melt inclusions from the Juan de Fuca Ridge, *Geochem. Geophys. Geosyst.*, *12*, Q12T11, doi:10.1029/2011GC003778.

Theme: Towards an Integrated View of Volcanic and Hydrothermal Processes on the Juan de Fuca Ridge
Guest Editors: W. S. D. Wilcock, J. F. Holden, J. B. Gill, and E. Baker

1. Introduction

[2] The compositions of melt inclusions have long been viewed as be unique sources of primary information on magmatic systems [*Anderson and Wright*, 1972; *Anderson*, 1974; *Roedder*, 1979; *Dungan and Rhodes*, 1978; *Sobolev and Shimizu*, 1993; *Sobolev et al.*, 1994; *Nielsen et al.*, 1995]. The processes that result in pockets of melt enclosed by a host crystal include fracture healing, dissolution followed by re-crystallization and enclosed hopper growth. Each of these processes will trap different populations of melts which may have distinct textures and different compositional relationship to the host [*Roedder*, 1979; *Kohut and Nielsen*, 2004; *Kent*, 2008]. In MORB melts, inclusions formed by enclosed hopper growth are by far the most common, and are generally considered the type most likely to preserve primitive compositions and to be in local equilibrium [*Kent*, 2008] and therefore we focused on this type of melt inclusion in this study. A primary advantage of such melt inclusions is that they have the potential to preserve the original range of composition generated in the mantle and lower crust [e.g., *Sobolev and Shimizu*, 1993; *Sours-Page et al.*, 1999; *Kohut and Nielsen*, 2004; *Kent*, 2008]. Improved access to more primitive compositions, allows construction of much more quantitative, textured models of petrologic processes in basaltic systems.

[3] Despite the premise that inclusions represent relatively unmodified melt compositions, both the composition of the melt inclusions and the host crystal may be influenced by the mechanisms by which inclusions are trapped and subsequently evolve. Therefore, it is critical to be able to identify and quantify the effects of any process specific to inclusion formation and evolution, which might drive the composition of the trapped liquids away from that of the ambient melt at the time of trapping [*Danyushevsky et al.*, 2002; *Cottrell et al.*, 2002]. These processes may be divided into entrapment and post-entrapment processes. Entrapment processes include boundary layer effects and the entrapment of anomalous melts and the diffusive modification of fast or slow doffing elements. Post-entrapment processes include post-entrapment crystallization and diffusive re-equilibration (either pre-eruptive or effects caused by re-homogenization). A number of investigations have been conducted over the past two decades, focused on documenting and understanding both the processes themselves, as well as their potential significance [e.g., *Qin et al.*, 1992; *Cottrell et al.*, 2002; *Danyushevsky et al.*, 2000, 2002, 2003; *Gaetani and Watson*, 2000, 2002; *Michael et al.*, 2002; *Kohut and Nielsen*, 2004; *Faure and Schiano*, 2005; *Goldstein and Luth*, 2006; *Rowe et al.*, 2007; *Baker*, 2008; *Kent*, 2008; *Portnyagin et al.*, 2008].

[4] Melt inclusions are present in phenocrysts from all MORB magma types, and to different degrees in olivine, plagioclase and clinopyroxene [e.g., *Sobolev and Shimizu*, 1993; *Gurenko and Chaussidon*, 1995; *Nielsen et al.*, 1995; *Sobolev*, 1996; *Saal et al.*, 1998; *Shimizu*, 1998; *Sours-Page et al.*, 1999, 2002; *Kohut and Nielsen*, 2004]. They are particularly abundant in high anorthite phenocrysts and megacrysts [*Nielsen et al.*, 1995; *Sours-Page et al.*, 1999, 2002; *Danyushevsky*, 2001; *Danyushevsky et al.*, 2002, 2003; *Kohut and Nielsen*, 2004; *Font et al.*, 2007]. This investigation focused on primary melt inclusions, whose textures are consistent with their formation during crystal growth. Inclusions interpreted as formed as a consequence of fracture healing or dissolution were excluded from the analysis. Such inclusions were identified by their elongate or irregular morphology or presence in lines that crosscut the zoning patterns of the phenocrysts [*Nielsen et al.*, 1995]. The majority (~95–98%) of the melt inclusions in these samples were either round or ellipsoidal in shape and/or present in concentric bands.

[5] Plagioclase provides some interesting opportunities and challenges as a host for melt inclusions. It is a common phenocryst phase in primitive MORB and often contains numerous melt inclusions. In addition, it is characterized by a low rate of diffusion for many elements [*Grove et al.*, 1984, 1992; *Giletti and Casserly*, 1994; *Giletti and Shanahan*, 1997;

Cottrell et al., 2002; *Costa et al.*, 2003; *Cherniak*, 2010]. Despite this, a number of studies have suggested that plagioclase-hosted inclusions are specifically prone to modification by processes such as boundary layer entrapment or diffusive equilibration [*Giletti and Casserly*, 1994; *Giletti and Shanahan*, 1997; *Nakamura and Shimakita*, 1998; *Cottrell et al.*, 2002; *Michael et al.*, 2002; *Danyushevsky et al.*, 2002; *Costa et al.*, 2003; *Baker*, 2008].

[6] Boundary layer entrapment refers to a syn-crystallization process wherein a boundary layer at the interface between the crystal and the liquid becomes depleted in the crystal components (e.g., Al and Sr in the case of plagioclase) and enriched in excluded elements (e.g., Ti and Mg). If such a layer is trapped in a melt inclusion [*Kohut and Nielsen*, 2004; *Baker*, 2008], the composition of the melt inclusion will differ from that of the host liquid. The extent to which the inclusion composition will differ from the host (which is the composition we are attempting to re-construct) will depend on the rate of crystallization and the diffusion rates of the melt components.

[7] Post entrapment re-equilibration is a process that occurs between the phenocrysts and either the melt inclusions, or the host magma. In either case, components diffuse through the crystal as the system attempts to adjust to changes in the ambient conditions. The rate at which re-equilibration occurs is different for different components and depends on time, distance and the partition coefficient and rate of diffusion of each component [*Cottrell et al.*, 2002].

[8] In this contribution we introduce a new approach to the study of the origin of melt inclusions wherein we focus on investigating the compositions of both inclusions and their host plagioclase. Our goal is to understand the degree to which the original melt compositions from which the phenocrysts formed are represented by the melt inclusions. In effect, we hope to answer the question "what part of the geochemical signal is most likely preserved, and under what circumstances." As frame of reference, we use the observed partitioning of trace elements to assess the degree of equilibrium between each inclusion and the host plagioclase. Equilibrium at the time of trapping between a melt inclusion and the host mineral is a primary requirement for a melt inclusion to be considered unmodified and to provide useful information. Most workers explicitly or implicitly assume that melt inclusions are trapped in chemical equilibrium with their host minerals, and numerical correction schemes for post entrapment crystallization and diffusive equilibration typically assume such initial equilibrium exists [e.g., *Sobolev and Chaussidon*, 1996; *Danyushevsky et al.*, 2000, 2002, 2003; *Kress and Ghiorso*, 2004; *Kent*, 2008]. However, the assumption of equilibrium between inclusions and their host is almost never tested or examined in detail.

[9] Plagioclase is particularly suitable for a test of the veracity of melt inclusion compositions and degree of local equilibrium as it has concentrations of several trace elements (Mg, Ti, Sr, etc.) that are sufficiently high to be accurately measured by in situ techniques with a high degree of spatial resolution. In combination with separate analysis of melt inclusions, the apparent partition coefficient of trace elements between mineral and host can be calculated and compared to existing partitioning models. Thus the analysis of the mineral host and inclusion provides a direct means to test the degree of local equilibrium between the two.

2. Ultra-depleted Plagioclase-Hosted Melt Inclusions

[10] A specific focus of this study is the origin of wide range of HFSE contents observed in MORB melt inclusions [e.g., *Nielsen et al.*, 2000; *Danyushevsky et al.*, 2002]. One of the persistent questions in MORB petrology has been the petrogenesis of anomalously low Ti (and other HFSE) concentrations in some melt inclusions hosted in anorthitic phenocrysts in MORB lavas [*Sinton et al.*, 1993; *Nielsen et al.*, 1995; *Sours-Page et al.*, 1999; *Danyushevsky*, 2001; *Michael et al.*, 2002; *Cottrell et al.*, 2002; *Sours-Page et al.*, 2002; *Danyushevsky et al.*, 2003]. The general characteristics of populations of high anorthite hosted inclusions include:

[11] 1. Major element compositions are relatively homogeneous compared to incompatible trace elements, particularly within individual phenocrysts.

[12] 2. The liquids are multiply saturated at low pressure ($\sim < 0.2$ GPa) with plagioclase, olivine and aluminous spinel [*Kohut and Nielsen*, 2003].

[13] 3. Minor and trace element (e.g., Ti, Zr, and REE) compositions are homogenous within individual phenocrysts, but more heterogeneous across different samples of the suite [*Sours-Page et al.*, 1999]. This is true for both naturally quenched and rehomogenized inclusions.

[14] 4. Ti, Fe and HFSE are depleted relative to elements inferred to have similar partitioning behavior during melting (e.g., REE) [*Sours-Page et al.*, 1999, 2002; *Nielsen et al.*, 2000].

[15] 5. Inclusion bearing, high anorthite phenocrysts are present in all major MORB magma types (E-MORB, N-MORB and T-MORB) [*Nielsen et al.*, 2000].

[16] 6. Inclusions in plagioclase are sometimes, but not always [*Sours Page et al.*, 2002] compositionally distinct from inclusions in coexisting olivine and spinel [*Danyushevsky et al.*, 2002]. In addition, plagioclase and olivine hosted spinels exhibit distinct compositional populations [*Allan et al.*, 1988].

[17] Discussion of the origin and significance of the patterns evident in Ti and other HFSE elements in melt inclusions in plagioclase-hosted inclusions has been particularly contentious. *Nielsen et al.* [2000] argued that at least some of the observed range of composition is related to mixing of the mantle derived MORB magmas with a partial melt of altered depleted harzburgite (which was inferred to be Cl-rich). *Michael et al.* [2002] proposed a model wherein the low Ti and HFSE contents in anorthite-hosted melt inclusions were generated by dissolution of plagioclase followed by channel diffusion of the incompatible trace elements from the matrix glass through the melt interface. The depleted character of the inclusions was attributed to relatively slow rate of diffusion of Ti, Zr, and the REE in basaltic melts (compared with alkalis).

[18] *Danyushevsky et al.* [2002] attributed the low Ti content of some melt inclusions to diffusive re-equilibration with the host phenocryst. He concluded that the process of re-homogenization of melt inclusions would have a direct effect on the minor and trace element contents that would be distinct from the compositions trapped during crystallization. Some minor and trace element contents were deemed to be robust with respect to the entrapment and rehomogenization process (MgO, Al_2O_3, CaO, Na_2O, and K_2O) whereas others (e.g., TiO_2, FeO, and SiO_2) were not. The degree to which they represent the original host/parent magma was inferred to be dependent on the inclusion size and residence time, with larger inclusions more likely to preserve the parental signal.

[19] *Cottrell et al.* [2002] modeled post-entrapment diffusive re-equilibration in the inclusion/host system using a time-dependant diffusion model. They assumed that the inclusion and host were initially out of equilibrium. Their model calculates compositional change in the inclusions as a function of time as they equilibrate. A first order prediction from this model, as well as the earlier work of *Qin et al.* [1992], is that the rate of re-equilibration and the size of the 'halo' or region in diffusive communication with a given melt inclusion will be highly dependent on the size of the inclusion as well as the partition coefficient and diffusivity of any given element.

[20] Our work aims to test these models by focusing on the distribution of Ti, Sr and several minor elements between plagioclase host and melt inclusions. The distribution of elements with distinctly different diffusion rates and partition coefficients (e.g., Ti versus Sr and K) within the plagioclase phenocrysts will be used as a means of determining the extent to which diffusive re-equilibration has affected the composition of the observed phenocryst/inclusion.

3. Geologic Setting and Samples

[21] Samples selected for this study cover a wide range of oceanic basalt geochemical compositions including normal, depleted, and enriched mid-ocean ridge basalts (D-MORB, N-MORB, and E-MORB). All samples contain large phenocrysts of plagioclase (≥2 mm) that range from $An_{83–92}$ and contain abundant melt inclusions. These samples were the subject of a previous investigation [*Sours-Page et al.*, 1999], during which melt inclusions were analyzed by ion probe.

[22] Samples were selected from the northern end of the 130 km long Endeavor Segment of the Juan de Fuca Ridge (JdF). The Endeavor Segment has an intermediate/slow half-spreading rate of ~29 mm/yr [*Karsten et al.*, 1986]. *Karsten et al.* [1986] further subdivided the Endeavor segment into the younger (<200 ka), 18-km wide, and sinistral Endeavor Offset. The intermediate MORB samples (#E-5 - station TT-170-72 - 47° 41.48′ 129° 16.74 [*Karsten et al.*, 1990]) was dredged on-axis, whereas the E-MORB (E-32 – station TT175–51 - 48° 05.22′ 129° 1.92′ [*Karsten et al.*, 1990]) was dredged within a few kilometers of the axis (and is designated as "On Axis" by *Karsten et al.* [1990]). D22–3 (48° 26.8′ 129° 2.6′ [*Cousens et al.*, 1995]) was collected from a small center at the southern end of West Valley. The host lava types are petrographically and compositionally similar to other plagioclase ultraphyric lavas found at other ridges (e.g., AMAR [*Frey et al.*, 1993]; SEIR [*Douglas-Priebe*,

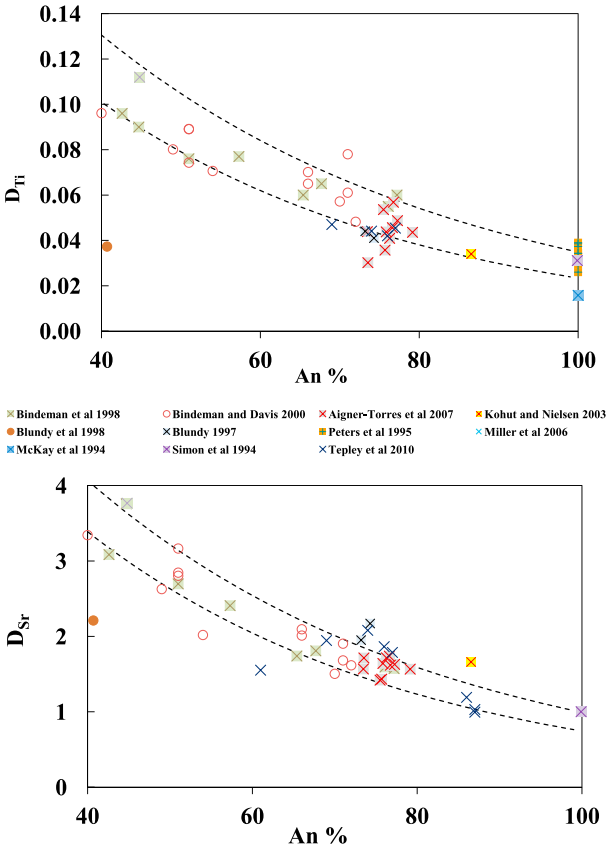

Figure 1. Experimentally determined plagioclase/melt Ti and Sr partition coefficients for basalts and basaltic analogs. Dashed lines are calculated maximum and minimum estimates from expressions of *Bindeman et al.* [1998]. Note the gap in the experimental data set above An_{80}. Other references include the experimental data of *McKay et al.* [1994], *Simon et al.* [1994], *Peters et al.* [1995], *Blundy* [1997], *Bindeman et al.* [1998], *Blundy et al.* [1998], *Bindeman and Davis* [2000], *Kohut and Nielsen* [2003], *Miller et al.* [2006], *Aigner-Torres et al.* [2007], and *Tepley et al.* [2010].

1998]; Galapagos Platform [*Sinton et al.*, 1993]; FAMOUS [*Langmuir et al.*, 1977]; EPR [*Hekinian and Walker*, 1987; *Batiza et al.*, 1989]; Chile Ridge [*Sherman et al.*, 1997]; Gorda Ridge [*Nielsen et al.*, 1995]).

4. Methods

4.1. Experimentally Determined Plagioclase-Melt Partition Coefficients

[23] To evaluate the degree to which melt inclusions represent the composition of the original melt, we evaluated the available experimental data on plagioclase/melt partition coefficients, updating the extensive review of *Bédard* [2006].

[24] Two observations are evident from the summary of experimental data for plagioclase (Figure 1). First is that the experimentally determined partition coefficients are negatively correlated with anorthite content (as predicted by *Blundy and Wood* [1991, 1994], *Bindeman et al.* [1998], and *Gaetani* [2004]). Second, there are no data for Ti in the range of An_{80} to An_{100}. Nevertheless, the existing data for Ti, are coherent and the data set for the lower An range ($<An_{80}$) conforms broadly to the empirical (calibrated to their experiments) partitioning relation proposed by *Bindeman et al.* [1998].

4.2. Melt Inclusion Rehomogenization

[25] Bulk samples of the Juan de Fuca Ridge lavas were coarsely crushed and the crystals were handpicked for rehomogenization. Rehomogenization temperatures (between 1200° and 1270°C) were determined based on the anorthite content of the feldspar host. The crystals were first heated to 1000°C for 20–30 min then held at their respective rehomogenization temperature. That re-homogenization temperature was determined by trial and error based on the anorthite content of the phenocrysts and the proximity of the melt inclusions to the olivine-plagioclase cotectic as established by olivine daughter crystals and calculated olivine/plagioclase equilibria (technique discussed in detail by *Nielsen et al.* [1995], *Sours-Page et al.* [1999], and *Nielsen* [2011]).

[26] We used a combination of analytical techniques to determine the chemistry of the melt inclusions and host plagioclase. Major and minor element compositions of plagioclase and melt inclusions were determined by electron microprobe. Trace element contents were determined only on the plagioclase, using laser ablation inductively coupled plasma mass spectrometry (LA-ICP-MS). No trace element data were collected for the melt inclusions as part of this investigation. However, as noted above, a number of melt inclusion analyses were collected on separate phenocrysts as part of the *Sours-Page et al.* [1999] investigation, and will be discussed below.

4.3. Electron Microprobe

[27] Major and trace element analyses for both melt inclusions and host plagioclase were performed using a CAMECA SX-100 electron microprobe at Oregon State University. BSE images were used to locate host/inclusion pairs for calculation of in situ partition coefficients. Melt inclusions were analyzed using an accelerating voltage of 15 kV, a sample current of 30 nA, and a defocused beam of 3–5 μm.

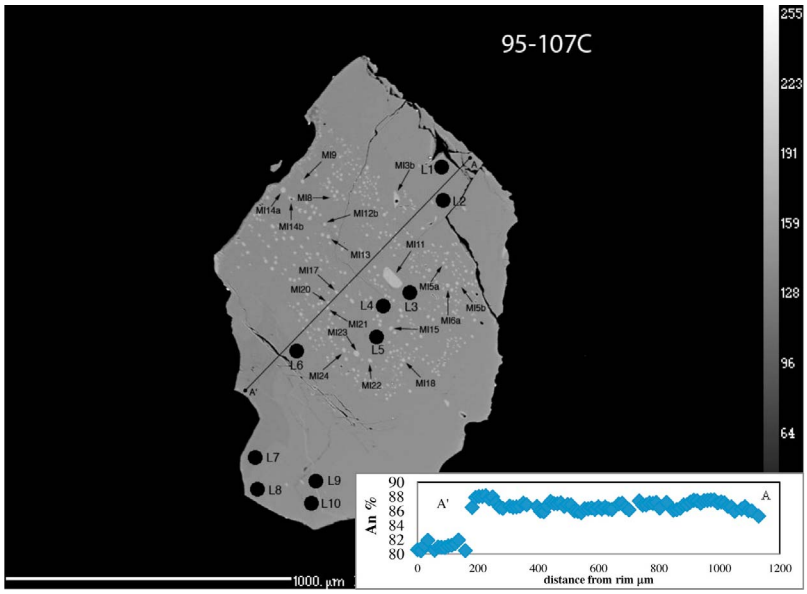

Figure 2. Example of backscattered electron images of plagioclase phenocryst and melt inclusions with locations of analyzed melt inclusions (labeled MIxx), and laser ICP-MS analyses (black circles labeled LX), and electron microprobe traverse in the inset (A-A′). Inset represents An% versus distance (μm) of the electron microprobe transects (data in Data Sets S1–S3). Note the presence of a homogenous core (based on distribution of MI) and rapid drop in An content near A′.

Time dependent intensity analysis was used to correct for element migration away from the beam (K and Na) and toward the beam (Si and Al). The following Smithsonian standards were used: USNM 115900 Lake County, OR labradorite for Si, Al, Na, and Ca; USNM 113498 Makaopui Lava Lake, Hawaii basaltic glass for Fe and Ti; USNM 122142 Kakanui, New Zealand augite for Mg; USNM 143966 microcline for K; USNM 104021 Durango, NM fluorapatite for P; and USNM117075 Tiebaghi Mine, New Caledonia chromite for Cr. Manganese was standardized with a synthetic pyroxmangite. In the plagioclase, full grain analytical traverses were performed using a 10 μm step size.

4.4. LA-ICP-MS

[28] Trace elements in the plagioclase were analyzed at the W.M. Keck Collaboratory for Plasma Spectrometry at Oregon State University on a NewWave DUV 193 μm ArF Excimer laser connected to a VG PQ ExCell Quadrupole ICP-MS. A stationary spot analysis was conducted using a pulse rate of 3–5 Hz and ablation duration of 45 s. The spot diameter was 45 μm. Background counts were measured for 30 s before ablation and subtracted from counts measured during ablation. Data were filtered to exclude signals that were less than background plus three standard deviations during ablation. USGS standard BCR-2G and NIST standard glass 612 were measured before and after each sample for calibration and drift correction, and to assess overall accuracy. As the internal standard, ^{43}Ca was used for data reduction on every sample. General analytical details are given by *Kent et al.* [2004]. Overall external reproducibility of trace element analyses was $\leq \pm$ 10–15% (2σ).

[29] LA-ICP-MS analyses typically involve multiple spots located 50–100 μm from the melt inclusion in question (Figure 2). This distance is sufficient to avoid small internal plagioclase growth rims related to any post entrapment crystallization, but close enough to reasonably include plagioclase grown during or immediately before or after inclusion entrapment.

[30] An additional complication for LA-ICP-MS analyses is the chance of hitting unexposed melt inclusions during progressive ablation. The crater produced by a single ablation was between 15 and 30 μm deep. In phenocrysts where inclusions are abundant this resulted in several analyses hitting unexposed inclusions. This effect was recognized by examining count rates of elements that are highly enriched in glass relative to plagioclase (Mg, Ba, and Ti).

5. Results

[31] Each crystal contains numerous melt inclusions with many phenocrysts exposing 10s to 100s of

Table 1 (Sample). Analyses of Melt Inclusions and Associated Host Plagioclase[a] [The full Table 1 is available in the HTML version of this article]

		Electron Microprobe Analyses of Plagioclase Hosted Melt Inclusions							
Sample	Crystal ID	MI #	SiO_2	TiO_2	Al_2O_3	FeO*	MnO	MgO	CaO
TT170-72 ID # E-5	host lava	50.03	1.61	14.99	9.38	0.15	7.52	12.23	2.68
TT-170	95-100B	14	50.45	0.62	16.88	7.92	0.15	8.41	12.38
TT-170	95-100B	10	50.19	0.66	16.78	7.98	0.15	8.59	12.40
TT-170	95-100B	11	50.71	0.57	16.24	8.05	0.16	9.07	12.26
TT-170	95-100B	7	50.38	0.85	16.56	7.89	0.14	8.86	12.49
TT-170	95-100B	6	50.73	0.65	17.62	7.55	0.15	8.31	12.61
TT-170	95-100B	4	50.77	0.59	16.41	7.67	0.13	8.66	12.44
TT-170	95-100B	3	50.64	0.68	16.52	8.02	0.16	8.61	12.42
TT-170	95-100B	1	50.72	0.67	16.69	8.23	0.17	7.83	12.20
TT-170	95-107B	12	49.83	0.73	16.99	7.59	0.12	9.29	12.14
TT-170	95-107B	9a-1	49.89	0.65	16.88	7.39	0.10	8.69	12.87
TT-170	95-107B	9a-2	49.89	0.66	16.91	7.61	0.15	8.53	12.70
TT-170	95-107B	9a-3	50.10	0.64	16.84	7.37	0.12	8.66	12.72
TT-170	95-107B	9b	49.69	0.70	16.73	7.20	0.11	8.80	12.98
TT-170	95-107B	10	49.71	0.73	16.85	7.30	0.09	9.06	12.67
TT-170	95-107B	8	49.74	0.70	16.81	7.18	0.15	8.82	13.12
TT-170	95-107B	7	49.97	0.69	16.60	7.24	0.15	8.80	13.08
TT-170	95-107B	3	49.50	0.72	15.93	7.50	0.13	9.05	13.44
TT-170	95-107C	11	50.74	0.34	17.11	7.90	0.12	7.93	12.39
TT-170	95-107C	12b	50.63	0.35	17.28	7.80	0.14	7.77	12.37
TT-170	95-107C	13	50.31	0.42	16.04	8.25	0.17	8.25	12.31
TT-170	95-107C	14a	50.76	0.40	16.64	8.07	0.17	8.04	12.30
TT-170	95-107C	14b	50.53	0.38	16.78	8.18	0.17	7.96	12.43
TT-170	95-107C	15	50.33	0.49	17.02	7.80	0.13	8.01	12.59
TT-170	95-107D	3	51.27	0.40	17.09	6.39	0.08	9.40	12.64
TT-170	95-107D	4	51.07	0.43	16.56	6.50	0.13	9.47	12.61
TT-170	95-107D	9	51.25	0.38	16.83	6.56	0.15	9.30	12.57
TT-170	95-107D	13	50.93	0.39	16.48	7.19	0.16	9.00	12.51
TT-170	95-107D	15	50.70	0.38	16.59	7.01	0.10	8.89	12.33
TT-170	95-107D	17	50.79	0.36	16.80	6.83	0.12	8.95	12.56
TT-170	95-107D	19	51.17	0.33	16.86	6.76	0.13	8.93	12.53
TT-170	95-107E	1	50.80	0.40	16.82	7.54	0.13	8.51	12.88
TT-170	95-107E	2	50.93	0.55	16.34	8.05	0.20	8.65	12.87
TT-170	95-107E	5	50.34	0.44	16.82	6.96	0.11	9.17	13.15
TT-170	95-107E	6	50.24	0.42	16.81	6.90	0.18	9.14	13.16
TT-170	95-107E	9	50.50	0.45	16.79	6.73	0.10	9.26	13.23
TT-170	95-107F	1a	51.18	0.53	16.34	7.31	0.15	8.63	13.11
TT-170	95-107F	3	50.70	0.59	16.38	6.85	0.15	8.89	13.20
TT-170	95-107F	4	50.73	0.64	16.36	6.75	0.13	9.01	13.06
TT-170	95-107F	9	49.30	0.57	16.09	6.37	0.15	8.67	14.47
TT-170	95-107F	10	51.04	0.60	16.41	6.80	0.17	9.06	13.27
TT-170	95-107F	15	50.46	0.62	16.39	6.53	0.14	9.24	12.94
Average									
Standard deviation									
D22-3	host lava		50.15	1.14	15.73	9.10	0.16	8.65	12.58
D22	95-74G	4	50.53	0.25	16.34	7.80	0.11	9.27	12.91
D22	95-74G	5	50.67	0.24	15.78	7.95	0.15	9.31	12.84
D22	95-74G	1	50.56	0.39	15.89	7.83	0.13	9.50	12.67
D22	95-74G	7	50.78	0.45	15.72	7.84	0.16	9.41	12.76
D22	95-74G	3	50.37	0.38	15.91	7.72	0.09	9.45	12.62
Average									
Standard deviation									
TT175-51 ID # E-32	host lava		50.16	1.72	15.48	8.98	0.16	6.95	11.90
E-32	95-113D	1	50.90	0.56	16.00	7.01	0.10	8.99	13.36

[a]Crystal ID # refers to specific crystal separated from sample #. MII# refers to melt inclusion number within a specific phenocryst. Mg# is calculated assuming 0.9 - FeO/(FeO+Fe2O3). Plag laser # refers to a specific LA-ICP analysis. An % is the anorthite content of the host plagioclase content of the host plagioclase phenocryst taken 50-150 μm from the inclusion. A full set of analyses is provided in a the auxiliary material. D^{Ti} and D^{Mg} were calculated using melt inclusion/host pairs using laser ICP analyses of the feldpsars obtained proximal to the MI (edge of ablation pit >20 microns from inclusion edge).

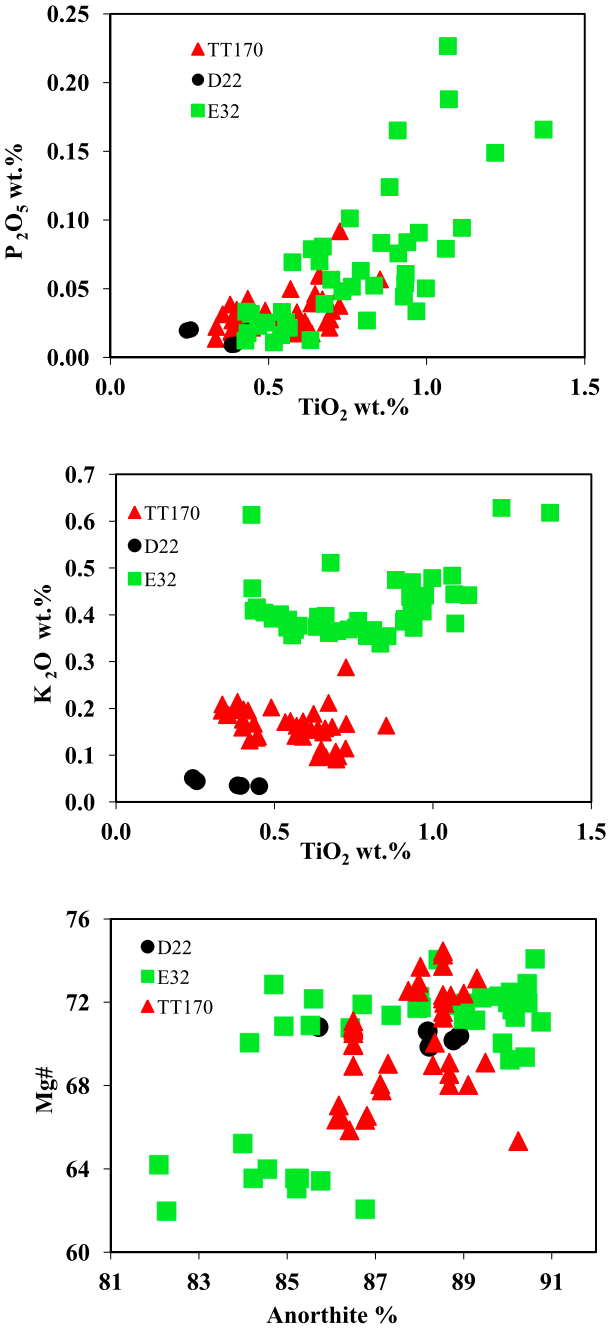

Figure 3. Major element composition of melt inclusion from three samples from the Juan de Fuca Ridge. (top) P_2O_5 correlation withTiO_2 (samples D22–3 from West Valley [*Cousens et al.*, 1995]; TT170–72 ID # E-5 [*Karsten et al.*, 1990]; TT175–51 ID # E-32 [*Karsten et al.*, 1990]), (middle) K_2O correlation with TiO_2 and (bottom) correlation of melt inclusion Mg# with host anorthite content proximal (~20 microns) to the inclusion. Note the correlation of P_2O_5 and TiO_2 compared to the plateau of K_2O relative to TiO_2. This pattern is consistent with the more rapid diffusion rate of K_2O compared to P_2O_5 or TiO_2.

inclusions at the surface (Figure 2). Melt inclusions range in size from two μm to 300 μm with the majority falling in the range of 10–50 μm (Figure 2). The rehomogenized melt inclusions exhibit some shrinkage bubbles although these are not uniformly present in inclusions from the same crystal. Inclusions range in shape from sub-spherical to ellipsoidal, often along growth bands with larger inclusions elongated parallel to the bands.

[32] Plagioclase crystals from each of the three samples studied exhibit remarkable internal homogeneity in An contents, typically exhibiting less than 2 An% variability over the entire grain. However, each grain is characterized by a distinct An content ranging from An_{83} to An_{91} (Table 1 and Data Sets S1–S3 in the auxiliary material).[1] All three samples exhibited a range of An contents in their crystal cargo, with the E-MORB (E-32) exhibiting the greatest range (Figure 3).

[33] Inclusions of spinel in plagioclase were rare and when present, were rounded/resorbed. No olivine inclusions were found within plagioclase in any of the samples we studied. However, there were phenocrysts of olivine present in all samples, but none in contact with the anorthitic plagioclase phenocrysts. These observations are consistent with petrographic observations of other plagioclase ultraphyric lavas [e.g., *Allan et al.*, 1988; *Sinton et al.*, 1993; *Nielsen et al.*, 1995], and suggest the possibility that they have different petrogenetic histories [*Lange et al.*, 2011].

5.1. Major Element Variations Between Inclusions

[34] In an investigation of the range of melt inclusion composition from these Juan de Fuca samples, *Sours-Page et al.* [1999] used the major elements contents of the melt inclusions to show the inclusions and phenocrysts are more primitive than their host lavas. However, the melt compositions (host lava and inclusions both) fall along a trend that is controlled by low-pressure olivine + plagioclase crystallization. They concluded that although the melt inclusions are genetically related to the host lava suite, they have undergone a lesser degree of low-pressure fractionation and mixing. They also observed that the phenocryst mode (at least 10:1 plagioclase:olivine) did not match the predicted crystallization mode (2:1 plagioclase:olivine), indicating

[1] Auxiliary materials are available at ftp://ftp.agu.org/apend/gc/2011gc003778.

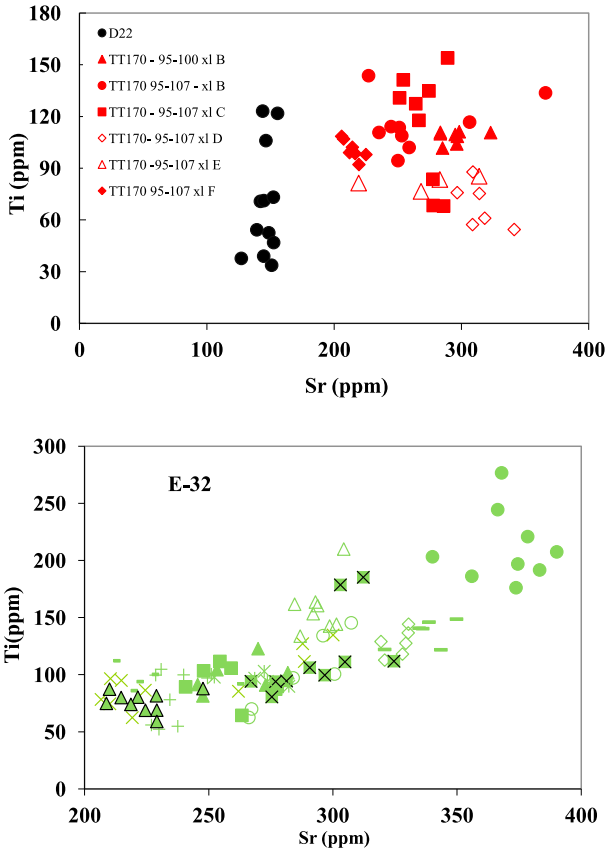

Figure 4. Ti and Sr composition for individual plagioclase phenocrysts from three Juan de Fuca ridge lavas (D22–3 from West Valley [*Cousens et al.*, 1995]; TT170–72 ID # E-5 [*Karsten et al.*, 1990]; TT175–51 ID # E-32 [*Karsten et al.*, 1990]). Individual points represent separate 60 μm diameter analyses of plagioclase, color coded by sample. Each symbol represents analyses of plagioclase from a different phenocryst from that individual sample. These analyses document a variety of patterns, consistent with variable degrees of diffusive re-equilibration (D22-3 with the greatest degree of re-equilibration, E-32 with the least).

a significant amount of crystal sorting during transport.

[35] Our new major element data and petrography on the same samples, agrees with those results (Figures 3 (top) and 3 (middle)). Major elements composition varies little between inclusions within individual grains, but can differ greatly from crystal to crystal even where crystals are from the same sample (Table 1 and Data Sets S1–S3). Magnesium numbers for the melt inclusions range from 62 to 74 (assuming 10% Fe^{+3}), are more primitive than their host lavas [*Sours-Page et al.*, 1999] and consistent with inclusions from other high anorthite hosted inclusions studied elsewhere.

[36] The TiO_2, P_2O_5, and K_2O contents are broadly correlated, with a general positive slope (Figures 3 (middle) and 3 (bottom)). However, inclusion K_2O tends to be uniform within each sample. The impression of a correlation is derived from a consideration of the total inclusion population from all samples. In contrast, the P_2O_5-TiO_2 data is correlated, although not linearly. It is important to note here that there is no evidence of high P_2O_5 or TiO_2 excursions within plagioclase or in plagioclase-hosted melt inclusions, similar to what has been observed in olivine for P_2O_5 [*Milman-Barris et al.*, 2008]. It is also important to note there is a general relationship of melt inclusion MgO with host anorthite content, which suggests that the inclusions do not represent anomalous melts present within the magma plumbing system, but are the same spectrum of melt compositions that eventually mix (after further crystal fractionation) to form the erupted host lava compositions. The average inclusion composition from each of the samples falls within their expected range predicted from the composition of their host lava, with sample D22 showing the most depleted signature, TT-170 falling within the intermediate range, and E-32 being the most enriched (Figure 3).

5.2. Minor and Trace Element Variation Within Plagioclase Phenocrysts

[37] The one distinctive aspect of this data set is analysis of the plagioclase host crystals. To obtain cross section of plagioclase compositions, a number of phenocrysts were analyzed in detail (Figures 2–5). The results (Figures 2–5) document a range of melt inclusion compositions within many individual crystals. Arguably more important, the data documents that the host plagioclases exhibits a wider range of minor (specifically Ti) and trace element composition (Sr and Ba) than represented by the melt inclusions in those same hosts. In detail, the patterns exhibited within each crystal vary, with some exhibiting a relatively coherent positive correlation of Ti versus Sr (e.g., TT170 95–107 xl B), and other crystals exhibiting a range of Ti and a narrow range of Sr (e.g., D22 and TT170 95–107 xl C) (Figure 4).

6. Discussion

6.1. Determination of in Situ Partition Coefficients

[38] The central premise of this investigation is that we can use the observed partitioning behavior of minor and trace elements between melt inclusions

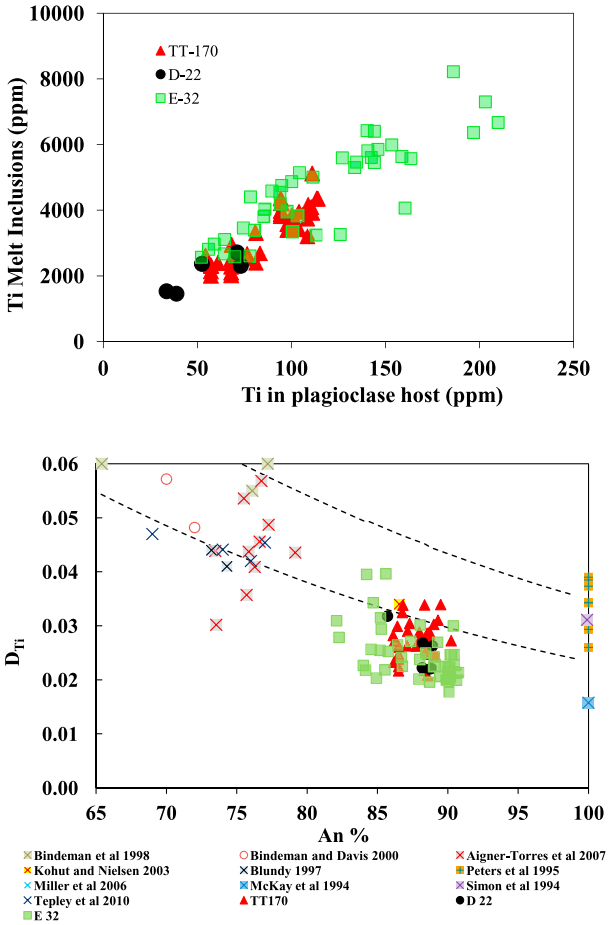

Figure 5. (top) Correlation of Ti in melt inclusions with Ti in host plagioclase. (bottom) Phenocryst/inclusion partition coefficients derived from this study compared to existing experimental determinations for Ti partitioning behavior. Note that the numbers reported here fall at the low end of the experimental values, and between those for natural terrestrial systems [*Aigner-Torres et al.*, 2007] and lunar or synthetic liquids [e.g., *McKay et al.*, 1994].

and their host phenocryst to test a number of hypotheses related to melt inclusion formation and the relationship between inclusions, their host crystals and the host lava suite. Once the inclusion and the associated host have been analyzed, we can calculate an apparent partition coefficient (D_{Ti} = $Ti_{plagioclase}/Ti_{Inclusion}$). If this value lies within the range predicted from partitioning experiments the melt inclusion and host can be inferred to be at local equilibrium with respect to that specific element.

[39] We begin our test by comparing our apparent partition coefficients with published experimental values for Ti (Figures 1 and 5). In the system examined here, the range of temperature and phase composition is fairly narrow. Therefore, we can expect that the measured partitioning would likewise exhibit a narrow range. Overall our values for D_{Ti} vary from an average of 0.024 ± 0.004 at An_{91}, to 0.30 ± 0.006 at An_{85} (average values for those specific An contents - relative standard deviations range up to 20% for individual samples (Table 1)). This degree of variation is similar to that expected from analytical uncertainty alone. The total range of D_{Ti} values that we measure is also less than that derived from most experimental studies, also due to the narrow range of temperature and composition represented in the system (Figures 5 and 6).

[40] The apparent values for D_{Ti} we obtain are also consistent with the trend defined by the available low pressure experimental determinations (Figure 5) for Ti partitioning between plagioclase and melt, falling between and slightly below the projected values from natural basaltic systems [e.g., *Aigner-Torres et al.*, 2007] and those obtained from synthetic and lunar systems [*Miller et al.*, 2006; *McKay et al.*, 1994]. As noted above, there are essentially no existing experimental determinations for systems that correlate precisely to the aluminous MORB magmas from which the anorthitic phenocrysts form. Nevertheless, in the absence of exact analogs, our results are consistent with the existing experimental data for Ti. Note also that this data set includes inclusion compositions that vary in TiO_2 content by a total factor of 3 within any sample (e.g., from 1800 to 5000 ppm for TT170 (Figures 4 and 5)) and individual crystals document a total range from 35 up to 200 ppm. Based on the restricted range of host/inclusion D_{Ti} (Figure 5, bottom), and the correlation with experimental data we conclude that there is no evidence for disequilibrium distribution of Ti between melt inclusions and host crystals. The extent of the variation in Ti and Sr with anorthite content is similar to that observed for D_{Ti}. We also emphasize that there is also no apparent relation between the measured D value and the size of the inclusion or the TiO_2 content of the trapped melt (Figure 6). The range of apparent D_{Ti} values increases as inclusion size decreases, however this can be attributed to the greater number of small inclusions analyzed.

6.2. Implications for Interpretation of Melt Inclusion Compositions

[41] The distribution of Ti between plagioclase and melt inclusions can provide an important test for models of melt inclusion formation. If we consider the case of entrapment of a boundary layer during melt inclusion formation [*Faure and Schiano*, 2005;

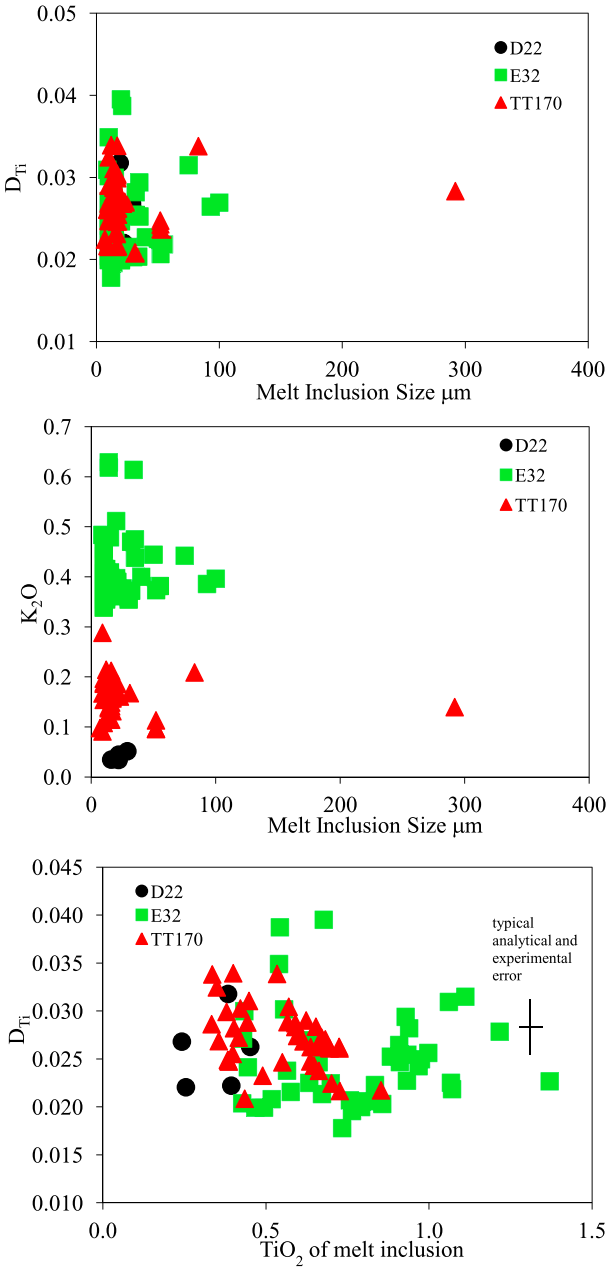

Figure 6. Correlation of (top) phenocryst/inclusion Ti partition coefficient and inclusion size, (middle) melt inclusion K_2O with melt inclusion size, and (bottom) host/inclusion D_{Ti} versus TiO_2 of melt inclusion. Note the lack of correlation with inclusion size, indicating that the inclusion did not trap a boundary layer.

Baker, 2008] the inclusion would trap a liquid that is anomalously high in incompatible elements, particularly those that have relatively slow diffusivities in basaltic liquid such as Ti [*Baker*, 2008], compared to the host liquid as a whole. *Baker* [2008] report enrichments of up to 50% in Ti content in experimentally produced melt inclusions. Such enrichments would translate to an anomalously low apparent D_{Ti}, compared to what one might expect based on experimental determinations. Such values would also be dependent on the size of the inclusion, because small inclusions would contain a higher proportion of the boundary layer. We would also expect inclusions with the highest TiO_2 contents to have the lowest apparent D_{Ti}, as the highest TiO_2 compositions would be expected to result from the greatest degree of boundary layer trapping. Given that we see no evidence for either anomalously low D values or variations between apparent D and inclusion size or inclusion TiO_2 content (Figure 6), we believe that boundary layer trapping has little discernable effect on the compositions of these inclusions. This conclusion is in accord with other studies of natural inclusions that find little evidence for trapping of boundary layers in melt inclusions in natural basaltic systems [*Nielsen et al.*, 1998; *Kuzmin and Sobolev*, 2004; *Kent*, 2008; *Severs et al.*, 2009] and in some experimental studies [*Kohut and Nielsen*, 2004; *Goldstein and Luth*, 2006].

[42] A second explanation for the patterns described above was presented by *Danyushevsky et al.* [2002], who proposed that the process of re-homogenization would have a significant effect on the major element composition of the inclusions, and would be correlated to inclusion size. However, a lack of correlation with inclusions size (Figure 6) indicates that, even though the issue of overheating, and heating trajectory may be important in a broad sense, the low Ti values exhibited by some of the plagioclase hosted inclusions and their host phenocrysts cannot be explained by the re-homogenization process. This has been independently affirmed in a separate study of plagioclase hosted inclusions [*Nielsen*, 2011].

[43] As described above, *Michael et al.* [2002] proposed a scenario wherein rapid dissolution of feldspar phenocrysts would create a boundary layer of plagioclase rich melt. Elements with different diffusivities would move into that layer at different rates, resulting in relatively enrichment of rapidly diffusing elements (e.g., Sr, K) and depletion in slow diffusing elements (e.g., Ti, HFSE). Entrapment of that interface would preserve a variably re-equilibrated melt composition that was not in equilibrium with the host plagioclase. That adjacent crystal would not be in equilibrium with the trapped melt, resulting in a high apparent D_{Ti}. This is not observed in our data set; there is no systematic correlation between apparent D and TiO_2 content (Figure 6). From this we argue that this specific trapping

mechanism has not been responsible for forming the inclusions in this study, and given that *Michael et al.* [2002] observed the low HFSE composition in only a small proportion of their own inclusions hosted in a single crystal, is probably only locally significant at best. Overall our data support a model whereby low HFSE melt inclusions form in equilibrium with host plagioclase, and by extension these represent real melts present within MORB systems.

[44] *Cottrell et al.* [2002] proposed a model of diffusive re-equilibration between inclusions and host that predicted a greater impact for faster diffusing elements such as K and Sr, and for smaller melt inclusions. Specifically, for any group of incompatible elements, elements that are fast diffusing within plagioclase and/or are more compatible (e.g., Sr, Eu in plagioclase) should exhibit lower variance among melt inclusions, and lesser degrees of zoning in phenocrysts. Observations of natural plagioclase hosted melt inclusion suites show anomalously low variance for Sr and Eu [*Cottrell et al.*, 2002; *Kent*, 2008] but not for HFSE. It is conceivable that the relatively constant apparent D we observe for Ti results from complete or near complete diffusive equilibration. However, if this were the case, then we would expect Ti contents in melt inclusions and associated plagioclase themselves to be homogenized with respect to Ti and all other elements that equilibrate at the same rate or faster, and to approach equilibrium with the external glass. This is not the case as Ti contents in melt inclusions and in individual plagioclase phenocrysts studied vary significant (Figures 4 and 5). Individual crystals show Ti variations of up to a factor of three (with D_{Ti} remaining broadly constant), and show variations that are close to the entire range of Ti variations observed in plagioclase from this study (e.g., Figure 4).

[45] Note that our data does not rule out diffusive equilibration of "faster" elements than Ti. The relatively small range of values for K_2O compared to P_2O_5 and TiO_2 within melt inclusions are consistent with some degree of diffusive equilibration of K. This is consistent with the more rapid rate of K diffusion in plagioclase [*Giletti and Shanahan*, 1997; *Cottrell et al.*, 2002; *Cherniak*, 2010] (Figure 3). Diffusive re-equilibration is also supported by the trace element concentrations measured in individual phenocrysts. For example, the data for D22 exhibit a narrow range of Sr and a wide range of Ti (Figure 4), consistent with the higher D and faster diffusion rate for Sr. Such a result would be predicted for any component with a fact diffusion rate and where the phenocryst had a long residence time. If diffusion has only partly equilibrated a given inclusion suite we might also expect to find relations between the apparent partitioning between inclusion and host, and the size of the inclusion, as geometry plays an important role in determining the rate at which diffusive equilibration occurs [*Qin et al.*, 1992; *Cottrell et al.*, 2002]. There is no dependence of K_2O with inclusion size (Figure 6, bottom). The coherent correlation characterized by the phenocrysts of sample E-32 suggest that 1) they are components of an array of related melts and 2) those phenocrysts had a relatively short (compared to D22) residence time (time interval between crystallization and eruption). In effect, this evidence indicates that the range of Ti, Sr and Ba (Table 1) represent a measure of the original array of parent magmas in this system with only the most rapidly diffusing elements, e.g., K_2O, exhibiting evidence of diffusive re-equilibration (Figure 3). In addition, the characteristics of the array of data suggest that the melts associated with the plagioclase phenocrysts extend to much more depleted compositions than any we see at the surface. In light of the new data on the character of abyssal peridotites [*Salters et al.*, 2011; *Stracke et al.*, 2011] raises some important questions with respect to the connection of erupted magmas to their proposed source – and in the case of plagioclase phenocrysts, to materials that remain in residence in the lower crust. In effect, how do transport processes affect the sampling the components of mantle melting and crustal processing? In addition, our results suggest that great care must be taken in the interpretation of ratios of elements that have different rates of diffusion (e.g., K/Ti). In the case of the samples reported on here, melt inclusions from D22 and TT170 exhibit a range of K_2O /TiO_2 that brackets that of the host lavas. In contrast, inclusions from E-32 exhibit a range of values that is, on average, lower than the host (Table 1).

[46] These results clearly raise as many questions as they answer. An ongoing study of the Sr isotopes of these phenocrysts and their host lava [*Lange et al.*, 2011] is targeted at further constraining the relationship between them, and ultimately the character of the array of magmas present at the site of plagioclase crystallization, presumed to be the lower crust.

[47] An alternative scenario to diffusional equilibration for Sr or K is that their values in melt and plagioclase were "buffered" by interaction with the lower crust prior to melt inclusion entrapment.

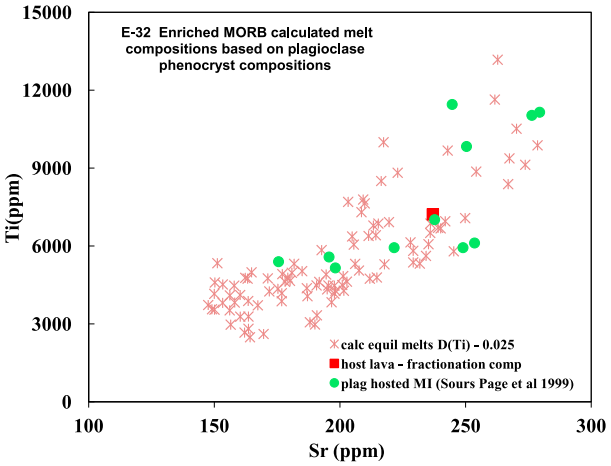

Figure 7. Comparison of melt compositions calculated from plagioclase phenocryst compositions with melt inclusions from Juan de Fuca E-MORB E-32 from *Sours-Page et al.* [1999]. The host lava composition has been corrected for ~30% fractional crystallization to the average MgO of the melt inclusions. The data from *Sours-Page et al.* [1999] was obtained from separate phenocrysts from those represented by the calculated melt compositions. This comparison can only be made on samples where there is a reasonable presumption that the phenocrysts, inclusions and the host lava are co-genetic.

Discrimination of these two scenarios requires that we know the initial state of the liquid, which we do not. However, an approximation may be made based on the maximum observed range in values if one has a number of different elements with different diffusion rates and similar partition coefficients. Unfortunately, the data set reported on here does not have sufficient range (in elemental behavior) to address this specific question quantitatively. Addressing this problem will involve collecting a wider range of compositional and isotopic data from the phenocrysts, melt inclusions and host lavas [*Lange et al.*, 2011].

7. Petrologic Context of Anorthitic Phenocrysts

[48] One of the challenges of working with melt inclusions is accommodating the perspective that they represent melts trapped during anomalous periods of crystal growth [*Kohut and Nielsen*, 2004; *Hammer*, 2008]. There remains a question as to the degree to which they are truly representative of the magmatic evolutionary trends of the system, regardless of the degree of post entrapment modification. In effect, we are left with the task of demonstrating that the crystals, trapped liquids, and host magma are all part of the same petrologic system. We have approached this problem by collectively considering the relationship of the crystal composition, the host/inclusion partition coefficients described above, and independently analyzed melt inclusion and host lava compositions.

[49] Phenocryst zoning profiles, particularly when combined with inclusion data, offer the advantage that they may preserve a more complete picture of the processes that generate the magmatic suite [e.g., *Kent*, 2008]. To successfully use trace element contents of phenocrysts together with liquid trends defined by inclusions and lavas as indicators of process, we must know the partitioning behavior of appropriate elements. There are significant limitations to partitioning models for plagioclase as applied to high An plagioclase in MORB (see above). However, as a proof of concept, we make an initial attempt using available data.

[50] The goal of this analysis is to evaluate the degree to which the anorthitic feldspars from the specific plagioclase phyric E-MORB studied above were in equilibrium with their melt inclusions and the associated lava suite. To test this we have calculated equilibrium melts from the minor and trace element contents of feldspar phenocrysts, using partition coefficients from our analysis and the literature, and have compared these compositions to melt inclusions from the same sample, and to the host lava. To make this an independent evaluation, we compared the calculated compositions to melt inclusions determined in a separate study, from separate phenocrysts, but from the same hand sample [*Sours-Page et al.*, 1999]. Those data were not used in the calculation of the apparent partition coefficients. Such a comparison is relevant only in cases where the phenocrysts appear to represent a coherent, genetically related population (e.g., sample E-32 (Figure 4, bottom)). In other cases, where the population of phenocrysts is diverse (e.g., sample TT170 (Figure 4, top)) one would not expect that the population of inclusions would necessarily be consistent with population of phenocrysts or with the host lava.

[51] The partition coefficients used were, for Ti, based on the phenocryst/inclusion ratios determined from that specific sample Ti ($D_{Ti} = 0.025$) and for Sr, based on projected values derived from experimentally determined partition coefficients (Figure 1; $D_{Sr} = 1.4$). The calculated equilibrium liquids (Figure 7), calculated from the plagioclase phenocrysts compositions (Table 1) exhibit complete

overlap (red crosses) with the melt inclusions (green circles) calculated from the *Sours-Page et al.* [1999] melt inclusion data collected from different phenocrysts from the same sample. Therefore, the inclusion compositions, their host phenocrysts and their host lavas represent a set of materials that are in general equilibrium (obviously the range of values means that no individual inclusion or crystal is in equilibrium with all materials). In addition, although the range of melt compositions inverted from phenocrysts overlaps the highest Ti and Sr values, it also extends to even lower Ti and Sr values than observed in the melt inclusions. This suggests that some of the feldspars formed from melts that are even more depleted (have lower incompatible elements) than the most depleted melt inclusions.

[52] The consequences of these calculations are relevant to the long-standing controversy regarding the petrogenesis of the Ti- and other HFSE-depleted melt inclusions common to plagioclase phenocrysts from this class of high Al MORB. Our results document that some of the inclusions and their host feldspars are highly depleted with respect to Ti and are real features of the melts that crystallize plagioclase. However, the range of Ti extends up to and above values we can infer to be in equilibrium with the host suite. This supports the conclusion that these feldspar phenocrysts crystallized from an array of magmas that includes both those characterized by extreme depletions in Ti and other HFSE, as well as more enriched components.

[53] This conclusion is in contrast to those of the interpretations of *Danyushevsky et al.* [2002] with regards to the different composition of spinel and plagioclase hosted melt inclusions in close association. The details of spinel – melt partitioning of Ti and the HFSE for these compositions is beyond the scope of this study. Nevertheless, the correlation of the calculated liquids based on plagioclase compositions and inferred experimental partition coefficients with both the host suite and the melt inclusion population is consistent with a genetic relationship (in these cases at least). This conclusion almost certainly varies from sample to sample, dependent on the provenance of the phenocrysts (e.g., the degree to which the crystals are xenocrystic versus autocrystic). In addition, the relationship between the observed phenocrysts (plagioclase, spinel and olivine) remains an open question. *Danyushevsky et al.* [2002] presumed that the phenocrysts represented an equilibrium assemblage (e.g., they all grew from the same liquid at the same time). However, the absence of high An plagioclase inclusions in olivine, or olivine inclusions in high An plagioclase, together with the resorbed texture of most spinel inclusions in plagioclase and the different population of spinel compositions in olivine and plagioclase [*Allan et al.*, 1988] suggests that the relationship may be more complex, and should be the subject of additional analysis. Regardless, we agree with *Danyushevsky et al.* [2002] that some of the major element patterns (specifically Al and perhaps Fe) were altered by post-entrapment re-equilibration and are a less robust signal than other components. Even though re-homogenization of the inclusions can eliminate most of those effects, major elements are somewhat susceptible to over and under heating. In contrast, incompatible minor and trace element contents are less sensitive, as indicated by comparison of naturally quenched and experimentally re-homogenized inclusions [*Nielsen*, 2011].

8. Conclusions

[54] This investigation focused on the relationship between the phenocryst composition and the melt inclusions trapped within them. Our goals in this study were **(i)** to evaluate the degree to which the melt inclusions represent the original trapped liquid (versus the product of entrapment or post-entrapment processes) and **(ii)** to use these analyses as a framework within which to evaluate whether the magmas that produce unusually anorthitic plagioclase belong to the mainstream of MORB magmas.

[55] To test these models, we examined the range of minor and trace elements composition in a number of melt inclusions and their plagioclase hosts. These are the observations we have made:

[56] 1. The Ti content of plagioclase from plagioclase ultra-phyric MORB lavas exhibits an even greater range of composition than that exhibited in the melt inclusions.

[57] 2. The observed variation in Ti in plagioclase is correlated with the Ti in the melt inclusions, exhibiting partitioning behavior similar to that predicted by experimental data.

[58] 3. There is no evidence that a trapped boundary layer represents a major part of the melt inclusion signal for plagioclase-hosted inclusions. In addition, such a process does not explain the observed low Ti contents observed in plagioclase-hosted inclusions.

[59] 4. Plagioclase hosts are equally depleted as the inclusions, suggesting that no depleted boundary

layer effect played a major role in the formation of the inclusions (e.g., *Michael et al.*'s [2002] model).

[60] 5. Each crystal appears to have a distinct history, and each sample contains a complex crystal cargo of phenocrysts. This is consistent with the findings of other investigators working on similar ultra-phyric samples [e.g., *Cordier et al.*, 2007; *Font et al.*, 2007; *Hellevang and Pedersen*, 2007].

[61] 6. Some individual crystals exhibit a narrow range of concentration for fast diffusing elements (e.g., Sr, K) in both melt inclusions and host feldspars, while exhibiting a wide range for slower diffusing elements (e.g., Ti). This is consistent with the model of *Cottrell et al.* [2002] for post-entrapment diffusive re-equilibration. In addition, the diffusive re-equilibration of K, complicates the use of K/Ti ratios to interpret the patterns observed in terms of the metrics normally used for erupted lavas.

[62] Considered collectively, our observations are consistent with a model wherein anorthitic feldspars in MORB represent the product of a combination of processes dependent on the specific transport history of their host. In each case, the range of phenocrysts represents a measure of the array of magmas present at the time of plagioclase crystallization – modified to different degrees by diffusive re-equilibration. However, that process cannot explain the extremely low values for Ti, which may represent a depleted component that is rarely sampled in the erupted lavas. This is consistent with a growing data set that indicates that parts of the mantle are characterized by highly depleted isotopic and trace element contents [*Salters et al.*, 2011; *Stracke et al.*, 2011]. Identification of the precise petrogenetic relationship between the phenocrysts and their host will require additional trace element and isotopic constraints [*Nielsen*, 2011; *Lange et al.*, 2011]. Perhaps most important, our results indicate that whatever relationship exists, it is shared by both the plagioclase phenocrysts and their melt inclusions.

[63] Within the context of the magmas of the Juan de Fuca Ridge, our results suggest that the magma storage and transport system sample very different materials in different locations, both in terms of the mantle melts and in terms of the crystal cargo. Some lavas contain phenocrysts, and melt inclusions that are representative (or at least related to) of the parent magmas of the host lava (e.g., E-32) while others (e.g., D22) have been significantly modified by post entrapment re-equilibration, and may be technically considered xenocrystic. Nevertheless, information implicit in their modified patterns may yield important information on the magma transport and storage system.

Acknowledgments

[64] We wish to acknowledge the generosity of all our colleagues who freely gave us samples of plagioclase phyric basalts over the years. This work could not have been done without access to those samples, and the advice of many on where to look in the dim and dark recesses of our sample repositories. This work was supported by NSF grant OCE0927773.

References

Aigner-Torres, M., J. Blundy, P. Ulmer, and T. Pettke (2007), Laser ablation ICPMS study of trace element partitioning between plagioclase and basaltic melts: An experimental approach, *Contrib. Mineral. Petrol.*, *153*(6), 647–667, doi:10.1007/s00410-006-0168-2.

Allan, J. F., R. O. Sack, and R. Batiza (1988), Cr-rich spinels as petrogenetic indicators: MORB-type lavas from the Lamont seamount chain, eastern Pacific, *Am. Mineral.*, *73*, 241–255.

Anderson, A. T. (1974), Evidence for a picritic, volatile-rich magma beneath Mt. Shasta, California, *J. Petrol.*, *15*(2), 243–267.

Anderson, A. T., and T. L. Wright (1972), Phenocrysts and glass inclusions and their bearing on oxidation and mixing of basaltic magmas, Kilauea Volcano, Hawaii, *Am. Mineral.*, *57*, 188–216.

Baker, D. R. (2008), The fidelity of melt inclusions as records of melt composition, *Contrib. Mineral. Petrol.*, *156*(3), 377–395, doi:10.1007/s00410-008-0291-3.

Batiza, R., T. L. Smith, and Y. Niu (1989), Geological and petrologic evolution of seamounts near the EPR based on submersible and camera study, *Mar. Geophys. Res.*, *11*(3), 169–236.

Bédard, J. H. (2006), Trace element partitioning in plagioclase feldspar, *Geochim. Cosmochim. Acta*, *70*(14), 3717–3742, doi:10.1016/j.gca.2006.05.003.

Bindeman, I. N., and A. M. Davis (2000), Trace element partitioning between plagioclase and melt: Investigation of dopant influence on partition behavior, *Geochim. Cosmochim. Acta*, *64*, 2863–2878, doi:10.1016/S0016-7037(00)00389-6.

Bindeman, I. N., A. M. Davis, and M. J. Drake (1998), Ion microprobe study of plagioclase-basalt partition experiments at natural concentration levels of trace elements, *Geochim. Cosmochim. Acta*, *62*(7), 1175–1193, doi:10.1016/S0016-7037(98)00047-7.

Blundy, J. D. (1997), Experimental study of a Kiglapait marginal rock and implications for trace element partitioning in layered intrusions, *Chem. Geol.*, *141*, 73–92.

Blundy, J. D., and B. J. Wood (1991), Crystal-chemical controls on the partitioning of Sr and Ba between plagioclase feldspar, silicate melts, and hydrothermal solutions, *Geochim. Cosmochim. Acta*, *55*(1), 193–209, doi:10.1016/0016-7037(91)90411-W.

Blundy, J., and B. J. Wood (1994), Prediction of crystal-melt partition coefficients from elastic moduli, *Nature*, *372*, 452–454, doi:10.1038/372452a0.

Blundy, J., J. A. C. Robinson, and B. J. Wood (1998), Heavy REE are compatible in clinopyroxene on the spinel lherzolite

solidus, *Earth Planet. Sci. Lett.*, *160*, 493–504, doi:10.1016/S0012-821X(98)00106-X.

Cherniak, D. J. (2010), Cation diffusion in feldspars, *Rev. Mineral. Geochem.*, *72*, 691–733, doi:10.2138/rmg.2010.72.15.

Cordier, C., M. Caroff, T. Juteau, C. Fleutelot, M. Drouin, J. Cotton, and C. Bollinger (2007), Bulk-rock geochemistry and plagioclase zoning in lavas exposed along the northern flank of the Western Blanco Depression (North Pacific): Insight into open-system magma chamber processes, *Lithos*, *99*(3–4), 289–311, doi:10.1016/j.lithos.2007.06.009.

Costa, F., S. Chakraborty, and R. Dohmen (2003), Diffusion coupling between trace and major elements and a model for calculation of magma residence times using plagioclase, *Geochim. Cosmochim. Acta*, *67*(12), 2189–2200, doi:10.1016/S0016-7037(02)01345-5.

Cottrell, E., M. Spiegelman, and C. H. Langmuir (2002), Consequences of diffusive reequilibration for the interpretation of melt inclusions, *Geochem. Geophys. Geosyst.*, *3*(4), 1026, doi:10.1029/2001GC000205.

Cousens, B. L., J. F. Allan, M. I. Leybourne, R. L. Chase, and N. Van Wagoner (1995), Mixing of magmas from enriched and depleted mantle sources in the northeast Pacific: West Valley segment, Juan de Fuca Ridge, *Contrib. Mineral. Petrol.*, *120*, 337–357, doi:10.1007/BF00306512.

Danyushevsky, L. V. (2001), The effect of small amounts of H_2O on crystallization of mid-ocean ridge and backarc basin magmas, *J. Volcanol. Geotherm. Res.*, *110*(3–4), 265–280, doi:10.1016/S0377-0273(01)00213-X.

Danyushevsky, L. V., F. N. Della-Pasqua, and S. Sokolov (2000), Re-equilibration of melt inclusions trapped by magnesian olivine phenocrysts from subduction-related magmas: Petrological implications, *Contrib. Mineral. Petrol.*, *138*(1), 68–83, doi:10.1007/PL00007664.

Danyushevsky, L. V., A. W. McNeil, and N. V. Sobolev (2002), Experimental and petrological studies of melt inclusions in phenocrysts from mantle-derived magmas: An overview of techniques, advantages and complications, *Chem. Geol.*, *183*, 5–24, doi:10.1016/S0009-2541(01)00369-2.

Danyushevsky, L. V., M. R. Perfit, S. M. Eggins, and T. J. Falloon (2003), Crustal origin for coupled ultradepleted and plagioclase signatures in MORB olivine-hosted melt inclusions: Evidence from the Siqueiros Transform fault, East Pacific Rise, *Contrib. Mineral. Petrol.*, *144*(5), 619–637, doi:10.1007/s00410-002-0420-3.

Douglas-Priebe, L. M. (1998), Geochemical and petrogenetic effects of the South East Indian Ridge and the Amsterdam-St. Paul hotspot, Masters thesis, 233 pp., Oreg. State Univ., Corvallis.

Dungan, M., and J. M. Rhodes (1978), Residual glasses and melt inclusions in basalts from DSDP Legs 45 and 46: Evidence for magma mixing, *Contrib. Mineral. Petrol.*, *67*(4), 417–431, doi:10.1007/BF00383301.

Faure, F., and P. Schiano (2005), Experimental investigation of equilibration conditions during forsterite growth and melt inclusion formation, *Earth Planet. Sci. Lett.*, *236*(3–4), 882–898, doi:10.1016/j.epsl.2005.04.050.

Font, L., B. J. Murton, S. Roberts, and A. G. Tindle (2007), Variations in melt productivity and melting conditions along SWIR (70°E-49°E): Evidence from olivine-hosted and plagioclase-hosted melt inclusions, *J. Petrol.*, *48*(8), 1471–1494, doi:10.1093/petrology/egm026.

Frey, F. A., N. Walker, D. Stakes, S. R. Hart, and R. L. Nielsen (1993), Geochemical characteristics of basaltic glasses from the AMAR and FAMOUS Axial Valleys, Mid-Atlantic Ridge (36°–37°N): Petrogenetic implications, *Earth Planet. Sci. Lett.*, *115*(1–4), 117–136, doi:10.1016/0012-821X(93)90217-W.

Gaetani, G. A. (2004), The influence of melt structure on trace element partitioning near the peridotite solidus, *Contrib. Mineral. Petrol.*, *147*, 511–527, doi:10.1007/s00410-004-0575-1.

Gaetani, G. A., and E. B. Watson (2000), Open-system behavior of olivine-hosted melt inclusions, *Earth Planet. Sci. Lett.*, *183*(1–2), 27–41, doi:10.1016/S0012-821X(00)00260-0.

Gaetani, G. A., and E. B. Watson (2002), Modeling the major-element evolution of olivine-hosted melt inclusions, *Chem. Geol.*, *183*(1–4), 25–41, doi:10.1016/S0009-2541(01)00370-9.

Giletti, B. J., and J. E. D. Casserly (1994), Strontium kinetics in plagioclase feldspars, *Geochim. Cosmochim. Acta*, *58*(18), 3785–3793, doi:10.1016/0016-7037(94)90363-8.

Giletti, B. J., and T. M. Shanahan (1997), Alkali diffusion in plagioclase feldspar, *Chem. Geol.*, *139*(1–4), 3–20, doi:10.1016/S0009-2541(97)00026-0.

Goldstein, S. B., and R. W. Luth (2006), The importance of cooling regime in the formation of melt inclusions in olivine crystals in haplobasaltic melts, *Can. Mineral.*, *44*(6), 1543–1555, doi:10.2113/gscanmin.44.6.1543.

Grove, T. L., M. B. Baker, and R. J. Kinzler (1984), Coupled CaAl-NaSi diffusion in plagioclase feldspar: Experiments and applications to cooling rate speedometry, *Geochim. Cosmochim. Acta*, *48*(10), 2113–2121, doi:10.1016/0016-7037(84)90391-0.

Grove, T. L., R. J. Kinzler, and W. L. Bryan (1992) Fractionation of mid-ocean ridge basalt (MORB), in *Mantle Flow and Melt Generation at Mid-Ocean Ridges*, *Geophys. Monogr. Ser.*, vol. 71, edited by J. P. Morgan, D. K. Blackman, and J. M. Sinton, pp. 281–310, AGU, Washington, D. C.

Gurenko, A. A., and M. Chaussidon (1995), Enriched and depleted primitive melts included in olivine from Icelandic tholeiites: Origin by continuous melting of a single mantle column, *Geochim. Cosmochim. Acta*, *59*(14), 2905–2917, doi:10.1016/0016-7037(95)00184-0.

Hammer, J. E. (2008), Experimental studies of the kinetics and energetic of magma crystallization, *Rev. Mineral. Geochem.*, *69*(1), 9–59, doi:10.2138/rmg.2008.69.2.

Hekinian, R., and D. Walker (1987), Diversity and spatial zonation of volcanic rocks from the East Pacific Rise near 21°N, *Contrib. Mineral. Petrol.*, *96*(3), 265–280, doi:10.1007/BF00371248.

Hellevang, B., and R. B. Pedersen (2007), Magma ascent and crustal accretion at ultraslow-spreading ridges: Constraints from plagioclase ultraphyric basalts from the Arctic Mid-Ocean Ridge, *J. Petrol.*, *49*(2), 267–294, doi:10.1093/petrology/egm081.

Karsten, J. L., S. R. Hammond, E. E. Davis, and R. G. Currie (1986), Detailed geomorphology and neotectonics of the Endeavour Segment, Juan de Fuca Ridge: New results from Seabeam swath mapping, *Geol. Soc. Am. Bull.*, *97*(2), 213–221, doi:10.1130/0016-7606(1986)97<213:DGANOT>2.0.CO;2.

Karsten, J. L., J. R. Delaney, J. M. Rhodes, and R. A. Liias (1990), Spatial and temporal evolution of magmatic systems beneath the Endeavour Segment, Juan de Fuca Ridge: Tectonic and petrologic constraints, *J. Geophys. Res.*, *95*(B12), 19,235–19,256, doi:10.1029/JB095iB12p19235.

Kent, A. J. R. (2008), Melt inclusions in basaltic and related rocks, *Rev. Mineral. Geochem.*, *69*, 273–331, doi:10.2138/rmg.2008.69.8.

Kent, A. J. R., E. M. Stolper, D. Francis, J. Woodhead, R. Frei, and J. Eiler (2004), Mantle heterogeneity during the forma-

tion of the North Atlantic igneous province: Constraints from trace element and Sr-Nd-Os-O isotope systematics of Baffin Island picrites, *Geochem. Geophys. Geosyst.*, *5*, Q11004, doi:10.1029/2004GC000743.

Kohut, E. J., and R. L. Nielsen (2003), Low-pressure phase equilibria of anhydrous anorthite-bearing mafic magmas, *Geochem. Geophys. Geosyst.*, *4*(7), 1057, doi:10.1029/2002GC000451.

Kohut, E. J., and R. L. Nielsen (2004), Melt inclusion formation mechanisms and compositional effects in high-An feldspar and high-Fo olivine in anhydrous mafic silicate liquids, *Contrib. Mineral. Petrol.*, *147*(6), 684–704, doi:10.1007/s00410-004-0576-0.

Kress, V. C., and M. S. Ghiorso (2004), Thermodynamic modeling of post-entrapment crystallization in igneous phases, *J. Volcanol. Geotherm. Res.*, *137*(4), 247–260, doi:10.1016/j.jvolgeores.2004.05.012.

Kuzmin, D. V., and A. V. Sobolev (2004), Boundary layer contribution to the composition of melt inclusions in olivine, *Geochim. Cosmochim. Acta*, *68*, A544–A544.

Lange, A. E., F. J. Tepley III, R. L. Nielsen, and A. W. Burleigh (2011), *Variations in magma transport recorded by plagioclase ultraphyric basalts: Preliminary results from SWIR, Blanco and Juan de Fuca*, paper presented at 2011 Fall Meeting, AGU, San Francisco, Calif., 5–9 Dec.

Langmuir, C. H., J. F. Bender, A. E. Bence, G. N. Hanson, and S. R. Taylor (1977), Petrogenesis of basalts from the FAMOUS area: Mid-Atlantic ridge, *Earth Planet. Sci. Lett.*, *36*(1), 133–156, doi:10.1016/0012-821X(77)90194-7.

McKay, G., L. Le, J. Wagstaff, and G. Crozaz (1994), Experimental partitioning of rare earth elements and strontium-constraints on petrogenesis and redox conditions during crystallization of Antarctic Angrite Lewis Cliff 86010, *Geochim. Cosmochim. Acta*, *58*(13), 2911–2919, doi:10.1016/0016-7037(94)90124-4.

Michael, P. J., W. F. McDonough, R. L. Nielsen, and W. C. Cornell (2002), Depleted melt inclusions in MORB plagioclase: Messages from the mantle or mirages from the magma chamber?, *Chem. Geol.*, *183*(1), 43–61, doi:10.1016/S0009-2541(01)00371-0.

Miller, B. V., A. H. Fetter, and K. G. Stewart (2006), Plutonism in three orogenic pulses, Eastern Blue Ridge Province, southern Appalachians, *Geol. Soc. Am. Bull.*, *118*(1–2), 171–184, doi:10.1130/B25580.1.

Milman-Barris, M. S., J. R. Beckett, M. B. Baker, A. E. Hofmann, E. Morgan, M. R. Crowley, D. Vielzeuf, and E. Stolper (2008), Zoning of phosphorus in igneous olivine, *Contrib. Mineral. Petrol.*, *155*(6), 739–765, doi:10.1007/s00410-007-0268-7.

Nakamura, M., and S. Shimakita (1998), Dissolution origin and syn-entrapment compositional change of melt inclusion in plagioclase, *Earth Planet. Sci. Lett.*, *161*, 119–133, doi:10.1016/S0012-821X(98)00144-7.

Nielsen, R. L. (2011), The effects of re-homogenization on plagioclase hosted melt inclusions, *Geochem. Geophys. Geosyst.*, *12*, Q0AC17, doi:10.1029/2011GC003822.

Nielsen, R. L., J. Crum, R. Bourgeois, K. Hascall, L. M. Forsythe, M. R. Fisk, and D. M. Christie (1995), Melt inclusions in high-An plagioclase from the Gorda Ridge: An example of the local diversity of MORB parent magmas, *Contrib. Mineral. Petrol.*, *122*(1–2), 34–50, doi:10.1007/s004100050111.

Nielsen, R. L., P. J. Michael, and R. Sours-Page (1998), Chemical and physical indicators of compromised melt inclusions, *Geochim. Cosmochim. Acta*, *62*(5), 831–839, doi:10.1016/S0016-7037(98)00024-6.

Nielsen, R. L., R. E. Sours-Page, and K. S. Harpp (2000), Role of a Cl-bearing flux in the origin of depleted ocean floor magmas, *Geochem. Geophys. Geosyst.*, *1*(5), 1007, doi:10.1029/1999GC000017.

Peters, M. T., E. E. Shaffer, D. S. Burnett, and S. S. Kim (1995), Magnesium and titanium partitioning between anorthite and Type B CAI liquid: Dependence on oxygen fugacity and liquid composition, *Geochim. Cosmochim. Acta*, *59*(13), 2785–2796, doi:10.1016/0016-7037(95)00173-W.

Portnyagin, M., R. Almeev, S. Matveev, and F. Holtz (2008), Experimental evidence for rapid water exchange between melt inclusions in olivine and host magmas, *Earth Planet. Sci. Lett.*, *272*(3–4), 541–552, doi:10.1016/j.epsl.2008.05.020.

Qin, Z., F. Lu, and A. T. Anderson (1992), Diffusive equilibrium of melt and fluid inclusions, *Am. Mineral.*, *77*(5–6), 565–576.

Roedder, E. (1979), Origin and significance of magmatic inclusion, *Bull. Mineral.*, *107*, 487–510.

Rowe, M. C., A. J. R. Kent, and R. L. Nielsen (2007), Determination of sulfur speciation and oxidation state of olivine hosted melt inclusions, *Chem. Geol.*, *236*, 303–322, doi:10.1016/j.chemgeo.2006.10.007.

Saal, A., S. Hart, N. Shimizu, E. Hauri, and G. D. Lane (1998), Pb isotopic variability in melt inclusions from oceanic island basalts, *Polyn. Sci.*, *282*(20), 1481–1484.

Salters, V. J. M., S. Mallick, S. R. Hart, C. H. Langmuir, and A. Stracke (2011), Domains of depleted mantle: New evidence from hafnium and neodymium isotopes, *Geochem. Geophys. Geosyst.*, *12*, Q08001, doi:10.1029/2011GC003617.

Severs, M. J., J. S. Beard, L. Fedele, J. M. Hanchar, S. R. Mutchler, and R. J. Bodnar (2009), Partitioning behavior of trace elements between dacitic melt and plagioclase, orthopyroxene, and clinopyroxene based on laser ablation ICP-MS analysis of silicate melt inclusions, *Geochim. Cosmochim. Acta*, *73*(7), 2123–2141, doi:10.1016/j.gca.2009.01.009.

Sherman, S., J. Karsten, and E. Klein (1997), Petrogenesis of axial lavas from the Southern Chile Ridge: Major element constraints, *J. Geophys. Res.*, *102*(B7), 14,963–14,990, doi:10.1029/97JB00510.

Shimizu, N. (1998), The geochemistry of olivine-hosted melt inclusions in a FAMOUS basalt ALV519-4-1, *Phys. Earth Planet. Inter.*, *108*, 183–201.

Simon, S. B., S. M. Kuehner, A. M. Davis, L. Grossman, M. L. Johnson, and D. S. Burnett (1994), Experimental studies of trace element partitioning in Ca, Al-rich compositions: Anorthite and perovskite, *Geochim. Cosmochim. Acta*, *58*(3), 1507–1523.

Sinton, C. W., D. M. Christie, V. L. Coombs, R. L. Nielsen, and M. R. Fisk (1993), Near-primary melt inclusions in anorthite phenocrysts from the Galapagos Platform, *Earth Planet. Sci. Lett.*, *119*(4), 527–537, doi:10.1016/0012-821X(93)90060-M.

Sobolev, A. V. (1996), Melt inclusions in minerals as a source of petrological information, *Petrologiya*, *4*(3), 228–239.

Sobolev, A. V., and M. Chaussidon (1996), H_2O concentrations in primary melts from suprasubduction zones and mid-ocean ridges: Implications for H_2O storage and recycling in the mantle, *Earth Planet. Sci. Lett.*, *137*(1–4), 45–55, doi:10.1016/0012-821X(95)00203-O.

Sobolev, A., and N. Shimizu (1993), Ultra-depleted primary melt included in an olivine from the Mid-Atlantic Ridge, *Nature*, *363*, 151–154, doi:10.1038/363151a0.

Sobolev, A. V., A. A. Gurenko, and N. Shimizu (1994), Ultra-depleted melts from Iceland: Data from melt inclusion studies, *Mineral. Mag.*, *58A*, 860–861, doi:10.1180/minmag.1994.58A.2.183.

Sours-Page, R., K. T. M. Johnson, R. L. Nielsen, and J. L. Karsten (1999), Local and regional variation of MORB parent magmas: Evidence from melt inclusions from the Endeavour Segment of the Juan de Fuca Ridge, *Contrib. Mineral. Petrol.*, *134*(4), 342–363, doi:10.1007/s004100050489.

Sours-Page, R., R. L. Batiza, and R. L. Nielsen (2002), Melt inclusions as indicators of parental magma diversity on the Northern East Pacific Rise, *Chem. Geol.*, *183*(1–4), 237–261, doi:10.1016/S0009-2541(01)00384-9.

Stracke, A., J. E. Snow, E. Hellebrand, A. von der Handt, B. Bourdon, K. Birbaum, and D. Gunther (2011), Abyssal peridotite Hf isotopes identify extreme mantle depletion, *Earth Planet. Sci. Lett.*, *308*(3–4), 359–368, doi:10.1016/j.epsl.2011.06.012.

Tepley, F. J., III, C. C. Lundstrom, W. F. McDonough, and A. Thompson (2010), Trace element partitioning between high-An plagioclase and basaltic to basaltic andesite melt at 1 atmosphere pressure, *Lithos*, *118*, 82–94, doi:10.1016/j.lithos.2010.04.001.